

## Synthesis of L-cysteine-CdSe Quantum Dots for Optical Biosensing Applications

Thalfaa Rasheed Ajeel<sup>1\*</sup>, Manal Midhat Abdullah<sup>1</sup>, and Fadhel Mohammed Lafta<sup>2</sup>

<sup>1</sup>Department of Physics, College of Science, University of Baghdad, Baghdad, Iraq

<sup>2</sup>Department of Biology, College of Science, University of Baghdad, Baghdad, Iraq

\*Corresponding author: [thalfaa.rasheed@gau.edu.iq](mailto:thalfaa.rasheed@gau.edu.iq)

### Abstract

Cadmium selenide (CdSe) nanocrystals, modified with water-soluble L-cysteine and known as CdSe/Cys nanocrystals, were synthesized using L-cysteine as a stabilizing agent. This synthesis process ensured the formation of highly stable nanocrystals with desirable properties for various applications. The CdSe/Cys nanocrystals were carefully studied using advanced methods to understand their structure, composition, and optical features in detail. The peak that shows the preferred (111) orientation of L-cysteine-capped CdSe matches the usual core components, as indicated by the XRD pattern. On the other hand, the peaks at (220) and (311) are not as prominent. Photoluminescence (PL) spectroscopy was conducted to study the optical properties of the CdSe/Cys nanocrystals. The PL spectra's strong fluorescence emission showed these nanocrystals' excellent quantum efficiency. The emission peak was sharp and well-defined, highlighting the uniformity in size and composition of the synthesised nanocrystals. The study revealed the robust fluorescence of the spherical CdSe/Cys nanoparticles, with an average diameter of 2.3 nm. Modifying the surface of CdSe nanoparticles with cysteine improved their water solubility and biocompatibility.

### Article Info.

#### Keywords:

*CdSe Quantum Dots, L-cysteine, Biosensors, Nanomaterials, Optical Properties.*

#### Article history:

*Received: Jul.08, 2024*

*Revised: Nov. 09, 2024*

*Accepted: Nov.26, 2024*

*Published: Jun.01, 2025*

### 1. Introduction

The extensively studied cadmium selenide (CdSe) quantum dot (QD) is a prominent II–VI semiconductor QD with diverse applications in fields, such as photovoltaics, LEDs, sensors, photodynamic therapy, and biomarkers [1-7]. Their unique properties, stemming from quantum confinement, enable these applications [8]. With a tunable energy band gap across the visible spectrum, their size and shape can be modified during synthesis. Various researchers were reported distinct methods for producing CdSe QDs. Their synthesis was achieved through radiation chemical, hydrothermal, sonochemical, microwave-assisted, conventional chemical reduction, and photochemical techniques. The photochemical synthesis method is the most significant of these techniques as it does not require hazardous chemicals or strict laboratory conditions [9-15]. QDs have been surface passivated and stabilized using a range of capping agents, including biomolecules, such as polysaccharides, DNA, proteins, and amino acids, among others, to limit their development and boost their stability for various applications [16, 17]. Interestingly, thiol (-SH) group-containing compounds have been employed extensively for chalcogenide QD capping. For example, capping agents for CdSe, CdS, CdTe, and so on frequently use L-cysteine, an amino acid with a thiol (-SH) group [18-21]. Cysteine is an essential amino acid in proteins, recognized for its thiol group, which enables disulfide bond formation and imparts unique structural qualities. Its molecular structure, which includes amino, carboxyl, and thiol groups commonly found in proteins, makes cysteine an excellent model for research. The chemical structure of cysteine consists of a central carbon atom bonded to an amino group (NH<sub>2</sub>), a carboxyl group (COOH), a hydrogen atom, and a side



chain containing a thiol group ( $-SH$ ). The thiol group, attached to the  $\beta$ -carbon (the second carbon in the side chain), gives cysteine its unique properties, allowing it to form disulfide bonds. This thiol ( $-SH$ ) group enables cysteine residues in proteins to link together, contributing to protein structure and stability. Using L-cysteine as a capping agent, CdS/CdSe core-shell quantum dots were produced and employed as selective fluorescent probes for  $Cu^{2+}$  ions [22]. An innovative method was introduced for the effective synthesis of CdSe nanoparticles in aqueous solutions, with L-cysteine used for passivation [23]. The newly developed CdSe/L-cysteine quantum dots enable biological labelling in aqueous environments. An eco-friendly process for making color-tunable CdSe nanocrystals has been recorded, using ascorbic acid as a reducing agent and L-cysteine as a capping agent [24]. CdSe quantum dots demonstrated cytotoxic effects [25]. However, diverse biomolecules can effectively inhibit it by serving as surface passivating/capping agents [26, 27]. This work aims to synthesize and characterize L-cysteine-modified CdSe quantum dots to develop highly sensitive and specific optical biosensors.

## 2. Experimental Work

Various materials, including 99.9% pure sodium sulfide ( $Na_2SO_3$ ), cadmium chloride ( $CdCl_2$ ), selenium ( $Se$ ), and sodium sulfide ( $Na_2S$ ), were supplied from Sigma-Aldrich without further purification. CdSe colloids were synthesized by mixing  $CdCl_2$  (solution 1) and  $Na_2SeSO_3$  (solution 2) in a 2:1 ratio, with Se and Cd ions at concentrations of 0.02 and 0.04M, respectively. In a three-neck flask, the Cd solution (heated at  $60^\circ C$  for 30 minutes) was added first, followed by the Se solution (heated at  $90^\circ C$  for 3 hrs). Ammonium hydroxide was added to adjust the pH to 7.2–7.4, and argon gas was cycled through the mixture for 30 minutes to produce CdSe nanoparticles (CdSe-NPs). 60 mg L-cysteine was dissolved in 2 mL of  $0.1 \text{ mol L}^{-1}$  NaOH and added to 1 mL of  $1 \text{ } \mu\text{mol L}^{-1}$  CdSe QDs (as shown in Fig. 1) in DI water, then stirred for 60 minutes. After 30 minutes of treatment under room temperature, the organic phase was removed and the material was filtered through a  $0.2 \text{ } \mu\text{m}$  filter to create thin films for surface morphology analysis. The ligand exchange with cysteine was carried out in a biphasic approach by mixing QDs in diluted water with phosphate-buffered saline (PBS) and L-cysteine solution. The mixture was stirred vigorously, resulting in phase transfer from the organic to aqueous phase within 30 minutes. The QDs were then precipitated twice with ethanol, re-dissolved in PBS at pH 7.4, and analyzed. QD-Cys formed macroscopic aggregates overnight at room temperature. Storage at  $4^\circ C$  in the dark extended the stability of the samples for only 24 hrs. The aggregation was caused by ligand dissociation and spontaneous oxidation, leading to cysteine dimer formation. Nanoparticles were characterized by X-ray diffraction (XRD) and Fourier transform infrared spectroscopy (FTIR).

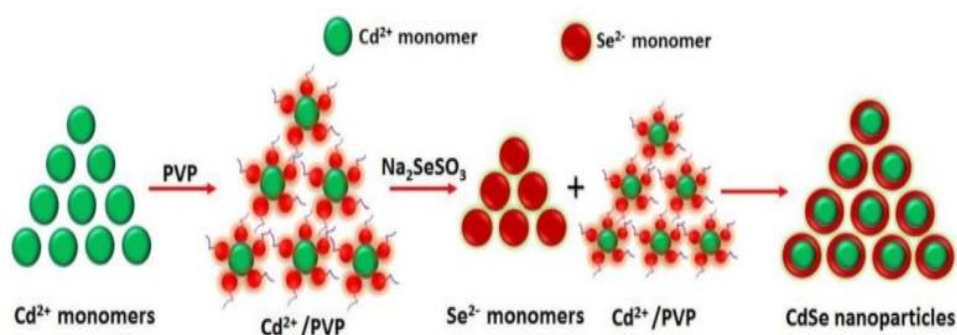


Figure 1: CdSe quantum dot synthesis [25].

### 3. Results and Discussion

#### 3.1. X-ray diffraction (XRD)

After capping with L-cysteine, the XRD peaks in Fig. 2 became clearly visible, confirming the successful capping of CdSe with L-cysteine. This observation is primarily attributed to the fact that the peak corresponding to the preferred (111) orientation of L-cysteine-capped CdSe coincides with the shared components of the core structure. The (111) peak is typically the most intense and represents the most stable and preferred crystalline orientation in the material. In contrast, the peaks at (220) and (311) show lower intensity, which can be attributed to the specific interactions between the L-cysteine molecules and the quantum dot core. These interactions may lead to the partial suppression or broadening of these peaks, resulting in lower intensity than that of the (111) peak. Such behavior highlights the influence of the capping agent on the structural and optical properties of the CdSe quantum dots, providing insights into the interaction between the capping molecules and the core material [28].

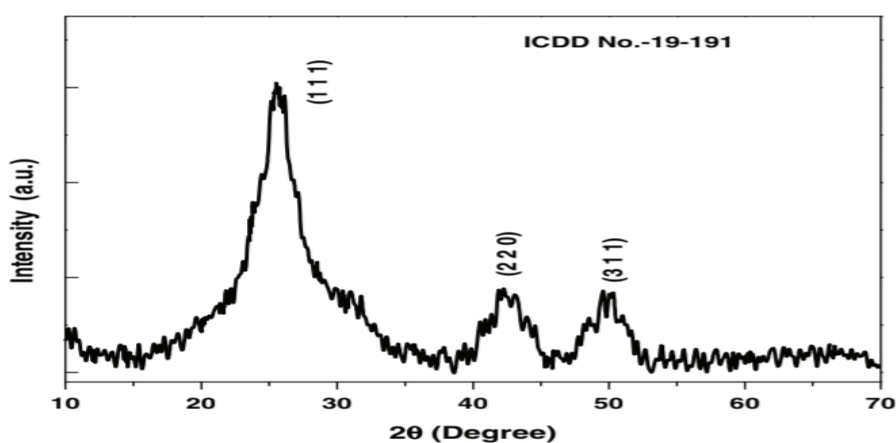


Figure 2: XRD pattern for CdSe capped L-Cysteine.

#### 3.2. Fourier-Transform Infrared (FTIR) measurements for CdSe with and without cysteine

FTIR spectroscopy was conducted to determine whether the powder sample of pure L-cysteine and L-cysteine-capped CdSe QDs had been capped. Fig. 3 shows the FTIR patterns for CdSe QDs and CdSe capped L-Cysteine. Peaks at 2800–3300  $\text{cm}^{-1}$  point to the  $\text{NH}_3$  group [29]. Three potential binding sites for L-cysteine are the carboxylate groups ( $\text{COOH}$ ), amino ( $\text{NH}_2$ ), and thiol ( $\text{SH}$ ). The confirmation of the zwitterionic form of L-cysteine is evident through the strong bands observed in the free form of L-cysteine at 1571  $\text{cm}^{-1}$ , attributed to the  $\text{NH}_2$  asymmetric bending, and at 1480 and 1385  $\text{cm}^{-1}$ , corresponding to the  $\text{COOH}$  asymmetric and symmetric stretching. The  $\text{NH}_3$  symmetric and asymmetric vibrations are indicated by the broad band at 2850 and 3130  $\text{cm}^{-1}$ , respectively, while the  $\text{NH}_3$  rocking vibration mode appears at 1120  $\text{cm}^{-1}$ , and the C–N stretching is depicted at 1045  $\text{cm}^{-1}$ . The vibrations S–H stretching and bending frequencies were detected at approximately 2580 and 960  $\text{cm}^{-1}$ , in that order. These S–H bands are absent from the FTIR spectra of CdSe capped by L-cysteine. This results from the S–H bond cleaving and the creation of a new Cd–S bond. This observation provides clear evidence of the surface bonding of L-cysteine with the CdSe QDs. The broad band in the 2760–3450  $\text{cm}^{-1}$  is found to be simple blue shifted to 2730–3430  $\text{cm}^{-1}$ . This is due to the N–H and N–H–O stretching, which may arise because of H-bonding in the alkaline pH of the reaction mixture. The characteristic frequency at 1385 and 1570  $\text{cm}^{-1}$

corresponds to COO—symmetric stretch and NH<sub>2</sub> asymmetric bending mode, respectively, are present in both spectra but have less intensity [30].

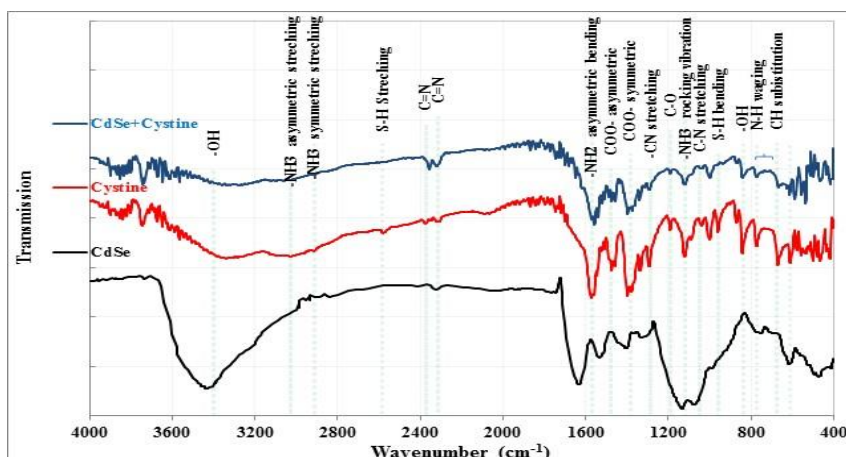


Figure 3: FTIR patterns for CdSe QDs and CdSe capped L-Cysteine.

### 3. 3. FESEM of CdSe with and without cysteine

The Field Emission Scanning Electron Microscopy (FESEM) images, shown in Fig. 4 (a and b), reveal the surface morphology of pristine CdSe quantum dots both with and without L-cysteine capping. The uncapped CdSe QDs exhibited spherical, uniform shapes with an average size of less than 10 nm, confirming the successful synthesis of CdSe quantum dots. The shell structure of CdSe was verified, and the surface of the sample appeared smoother compared to uncapped CdSe. When L-cysteine was added to the precursor solution, acting as a capping agent, the QDs became more uniform in size, and the average particle size increased to approximately 13 nm. The images, particularly in Fig. 4 (a), displayed aggregates of well-defined granules, suggesting that the QDs were closely packed together. The presence of L-cysteine not only improved the uniformity of the nanostructures but also had an impact on the overall size distribution of the particles. This indicates that L-cysteine plays a crucial role in stabilizing the QDs, preventing agglomeration, and enhancing their structural consistency. These findings are consistent with previous reports on the impact of surface passivation in controlling the morphology of CdSe QDs [31, 32].

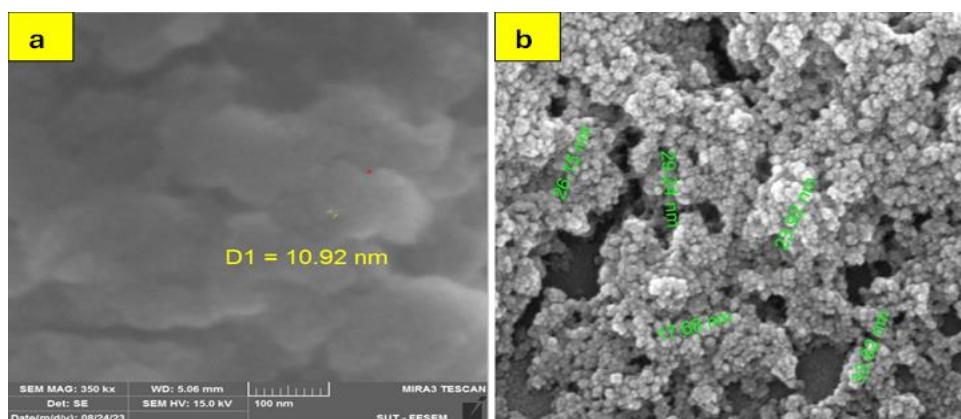
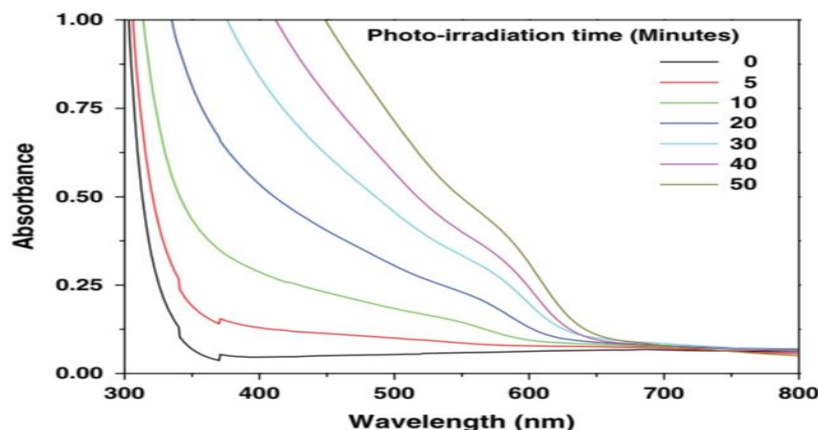


Figure 4: FESEM images of (a) CdSe QDs and (b) CdSe capped L-Cysteine.

### 3. 4. UV-Visible Absorption Studies

The UV-Vis absorption spectra were observed at different UV photo-irradiation durations to study how the absorption properties of the reaction mixtures evolve over time under light exposure. The duration of UV exposure can affect the size, surface properties,

and the formation of quantum dots, which influences the optical absorbance. This helps understanding the kinetics of quantum dot formation and the impact of irradiation time on their optical behavior, particularly when modifying the precursor and L-cysteine concentrations. Fig. 5 illustrates the absorption spectra obtained at different photo-irradiation periods for the solution with 0.3 mM L-cysteine, 2% (v/v) acetone, 2-propanol, and 1 mM of each precursor (Cd:Se = 1:1). The graph indicates an increase in absorbance with prolonged photo-irradiation [33].



**Figure 5:** UV-Vis absorption spectra of CdSe QDs synthesized with the precursors 1 mM each and L-cysteine 0.3 mM upon UV photo-irradiation at different time intervals.

This clearly confirms that there is a growth of CdSe QDs during photo-irradiation over time. The particle size of these quantum dots was determined using the Scherrer equation ( $D = k\lambda/B\cos\theta$ ). The parameters were set: K to 0.9,  $\lambda$  to 0.154 nm,  $\beta$  as the full width at half-maximum (FWHM), and  $\theta$  as the Bragg diffraction angle. The determined particle size ranges from 10 to 13 nm, which aligns well with the findings of the XRD analysis [28]. The reaction mixture comprising 1 mM [Cd(NH<sub>3</sub>)], 0.5 mM SeSO<sub>2</sub> (Cd:Se = 2:1), 0.3 mM L-cysteine, 2% (v/v) acetone, and 2-propanol has also undergone similar time-dependent absorption experiments as shown in Fig. 6. The creation of CdSe QDs was shown to be finished in ten minutes, while it took up to an hour for the reaction mixture comprising 1 mM of each precursor and 0.3 mM of L-cysteine to form fully.

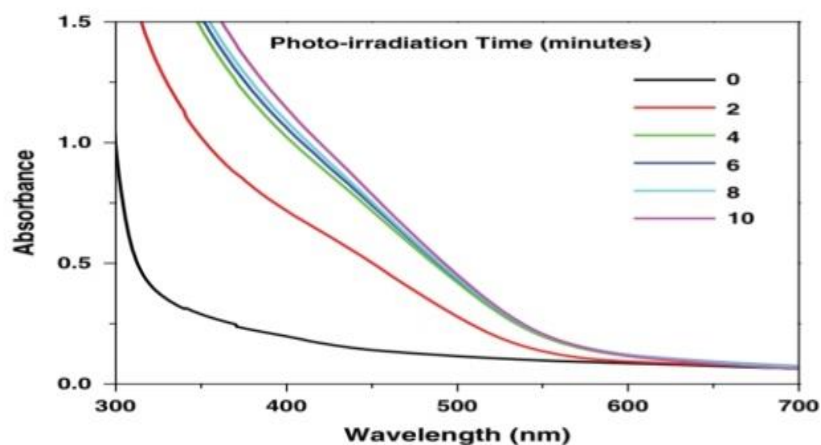


**Figure 6:** UV-vis absorption spectra of CdSe QDs synthesized with Cd, Se and L-cysteine 1, 0.5 and 0.3 mM, respectively, upon photo-irradiation at different time intervals.

It was noticed that the synthesis of CdSe QDs was complete even at an early time of light irradiation using 0.5mM[Cd(NH<sub>3</sub>)], 1mM SeSO<sub>2</sub> (Cd:Se=1:2), 0.3mM L-cysteine together with acetone and 2-propanol each 2%(v/v). However, the QDs, in this case, were unstable and aggregated, leading to the formation of larger particles in the solution. Thus, it became evident that CdSe QDs are better capped with L-cysteine at a greater Cd:Se ratio of 2:1, which increases the quantum dots stability. But at a lower Cd:Se ratio of 1:2, the QDs are weakly capped with L-cysteine, which makes it easy for them to aggregate to form larger particles. The FTIR investigations provided evidence that L-cysteine has a larger affinity for Cd than Se and that it attaches to the surface of Cd atoms, which explains these observations [33].

### 3. 5. Fluorescence Spectra

The fully-grown CdSe QDs fluorescence spectra were measured at room temperature with an excitation wavelength of 400 nm, as shown in Fig. 7. These CdSe QDs were synthesized using different reaction mixtures containing varied concentrations of precursors [Cd(NH<sub>3</sub>)] and SeSO<sub>3</sub>]: (a) 1 mM each (Cd:Se=1:1), (b) 1 and 0.5 mM (Cd:Se=2:1), (c) 1.25 and 0.5 mM (Cd:Se=2.5:1), and (d) 1.5 and 0.5 mM (Cd:Se=3:1) with 0.3 mM L-cysteine. The fluorescence spectra observed were broad, spanning from 480 to 750 nm, with a peak emission at 580 nm and a full width at half maximum of 150 nm. As the Cd:Se ratio in the reaction mixture increased, the emission intensity also increased. This phenomenon is probably due to enhanced surface passivation by L-cysteine with Cd, resulting in reduced surface trap states in the CdSe QDs and an elevation in the Cd content [34].

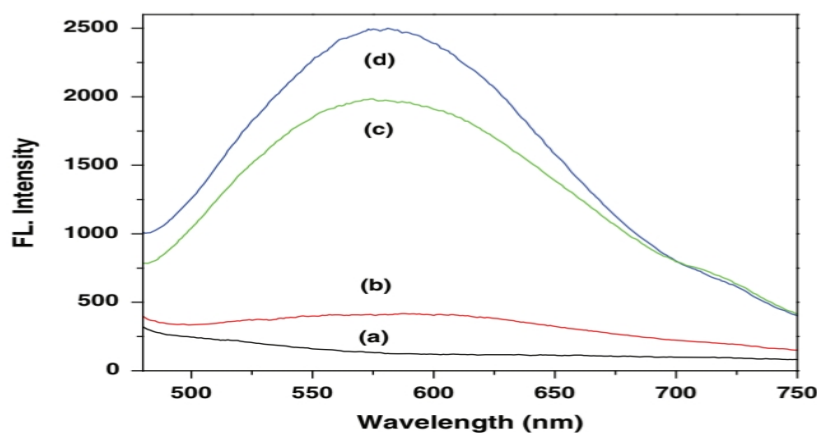


*Figure 7: Steady-state fluorescence spectra of CdSe QDs synthesized with different concentrations of the precursors, (a)1,1; (b)1, 0.5; (c) 1.25, 0.5; and (d)1.5, 0.5mM; andL-cysteine0.3mM upon UV photo-irradiation at room teperature.*

### 3. 6. In Vitro Toxicity Study

The CdSe QDs in this study were synthesized from two separate precursor compositions: (i) 1 mM [Cd(NH<sub>3</sub>)] and (ii) 1 mM [SeSO<sub>2</sub>]. When exposed to ultraviolet light, 0.5 mM SeSO<sub>2</sub> was used in water-based solutions containing 2% acetone and 2% propanol, with or without 0.3 mM cysteine. Using Chinese Hamster Ovary (CHO) epithelial cells, the biocompatibility of the CdSe QDs generated under various conditions was assessed by tracking the cells' vitality 48 hrs after they were added. Based on the data presented in Fig. 8, the cytotoxic effects were concentration-dependent when uncapped QDs with stoichiometry ratios of 1:1 and 2:1 were introduced to the cells. At all concentrations tested, the cytotoxicity of the 2:1 ratio was higher than that of the 1:1 ratio (1-4 g/ml). Capped QDs at concentrations up to 5 g/ml (1:1 and 2:1) showed no signs of toxicity. Despite observing a rise in toxicity with capped QDs at higher concentrations 10

g/ml, it remained significantly lower than that of the corresponding uncapped QDs. This difference is attributed to the smaller particle size in the 2:1 ratio, which is expected to yield a larger surface area and a higher quantity of Cd on the surface. Thus, when comparing a 1:1 to a 2:1 ratio, concentration and surface effects lead to increased cytotoxicity. Remarkably, quantum dots capped at 2:1 showed reduced cytotoxicity compared to those capped at 1:1, indicating the superior capping efficacy of L-cysteine at higher Cd concentrations. These findings align with known absorption and fluorescence characteristics of quantum dots. Therefore, capping is validated as an advanced approach to modify the toxicity of synthetic CdSe QDs, rendering them suitable for specific biological uses [35].

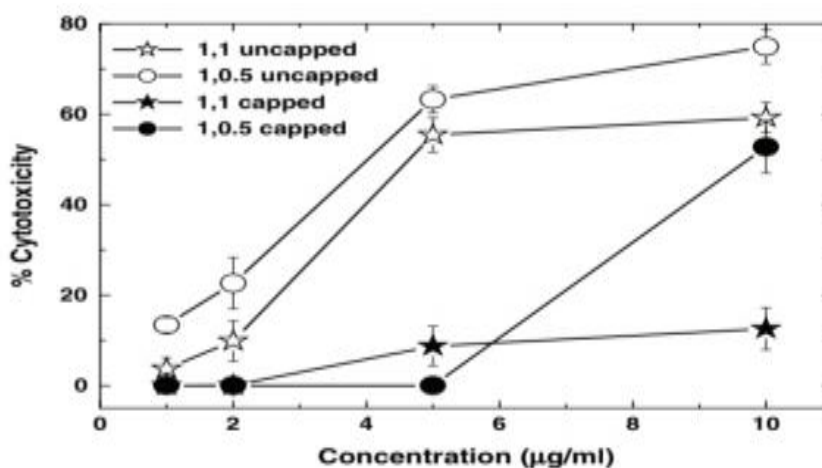


**Figure 8:** Cytotoxicity of CdSe QDs synthesized with different concentrations of the precursors and L-cysteine 0.3 mM under UV photo-irradiation, prepared under different conditions in CHO cells as determined by the MTT assay. Values are mean  $\pm$  SEM ( $n = 4$ ).

#### 4. Conclusions

The photochemical synthesis of L-cysteine-capped CdSe quantum dots in water was successfully achieved using very low precursor concentrations. A 2% (v/v) mixture of acetone and 2-propanol was added to the primary reagents, sodium selenosulfate and ammoniated cadmium sulfate. UV photoexcitation of acetone and hydrogen atom extraction from 2-propanol led to the formation of 1-hydroxy-2-propyl radicals, which then initiated the synthesis of CdSe quantum dots. The quantum dot formation process, including photo-irradiation, was completed in a few minutes. Varying the precursor concentrations in the reaction mixtures allowed for control over the room-temperature fluorescence of the quantum dots. Increasing the Cd concentration enhanced both the fluorescence intensity and the lifetime of the CdSe quantum dots, suggesting that L-cysteine molecules were more effective at passivating the surface of Cd-rich quantum dots. Furthermore, L-cysteine-capped CdSe quantum dots exhibited lower cytotoxicity compared to their uncapped counterparts.

#### Conflict of interest

Authors declare that they have no conflict of interest.

#### References

1. M. K. Ali, S. Javaid, H. Afzal, I. Zafar, K. Fayyaz, Q. U. Ain, M. A. Rather, M. J. Hossain, S. Rashid, K. A. Khan, and R. Sharma, *Envir. Res.* **232**, 116290 (2023). DOI: 10.1016/j.envres.2023.116290.
2. J. Sobhanan, J. V. Rival, A. Anas, E. Sidharth Shibu, Y. Takano, and V. Biju, *Adv. Drug Deliv. Rev.* **197**, 114830 (2023). DOI: 10.1016/j.addr.2023.114830.

3. B. Acharya, A. Behera, S. Behera, and S. Moharana, *Inorg. Chem. Communic.* **165**, 112492 (2024). DOI: 10.1016/j.inoche.2024.112492.
4. K. Koul, I. K. Jawanda, T. Soni, P. Singh, D. Sharma, and S. Kumari, *Arch. Microbio.* **206**, 158 (2024). DOI: 10.1007/s00203-024-03919-3.
5. Inamuddin, T. A. Rangrez, M. F. Ahmer, and R. Boddula, *Quantum Dots: Properties and Applications* (Millersville, USA, Materials Research Forum LLC, 2021).
6. C. Li and J. Lin, *Photofunctional Nanomaterials for Biomedical Applications* (China, John Wiley & Sons, 2025).
7. W. Guo, X. Song, J. Liu, W. Liu, X. Chu, and Z. Lei, *Nanomaterials* **14**, 1088 (2024). DOI: 10.3390/nano14131088.
8. F. P. García De Arquer, D. V. Talapin, V. I. Klimov, Y. Arakawa, M. Bayer, and E. H. Sargent, *Science* **373**, eaaz8541 (2024). DOI: 10.1126/science.aaz8541.
9. V. Singh, P. V. More, E. Hemmer, Y. K. Mishra, and P. K. Khanna, *Mat. Adv.* **2**, 1204 (2021). DOI: 10.1039/D0MA00921K.
10. J. Yu and R. Chen, *InfoMat* **2**, 905 (2020). DOI: 10.1002/inf2.12106.
11. Y. Al-Douri, M. M. Khan, and J. R. Jennings, *J. Mat. Sci. Mat. Elect.* **34**, 993 (2023). DOI: 10.1007/s10854-023-10435-5.
12. Y. Gao, Y. Liu, and D. Zou, *Envir. Chem. Lett.* **21**, 2399 (2023). DOI: 10.1007/s10311-023-01599-x.
13. G. Chatel and R. S. Varma, *Green Chem.* **21**, 6043 (2019). DOI: 10.1039/C9GC02534K.
14. G. N. Kokila, C. Mallikarjunaswamy, and V. L. Ranganatha, *Inorg. Nano Met. Chem.* **54**, 942 (2024). DOI: 10.1080/24701556.2022.2081189.
15. N. Jara, N. S. Milán, A. Rahman, L. Mouheb, D. C. Boffito, C. Jeffryes, and S. A. Dahoumane, *Molecules* **26**, 4585 (2021). DOI: 10.3390/molecules26154585.
16. Daphika s. Dkhar, R. Kumari, V. Patel, A. Srivastava, R. Prasad, R. Srivastava, and P. Chandra, *WIREs Nanomed. Nanobiotech.* **16**, e1998 (2024). DOI: 10.1002/wnan.1998.
17. N. R. S. Sibuyi, K. L. Moabelo, A. O. Fadaka, S. Meyer, M. O. Onani, A. M. Madiehe, and M. Meyer, *Nanoscal. Res. Lett.* **16**, 174 (2021). DOI: 10.1186/s11671-021-03632-w.
18. V. N. Mehta, M. L. Desai, H. Basu, R. Kumar Singhal, and S. K. Kailasa, *J. Molec. Liq.* **333**, 115950 (2021). DOI: 10.1016/j.molliq.2021.115950.
19. M. Sobiech, P. Bujak, P. Luliński, and A. Pron, *Nanoscale* **11**, 12030 (2019). DOI: 10.1039/C9NR02585E.
20. N. Wongkaew, M. Simsek, C. Griesche, and A. J. Baeumner, *Chem. Rev.* **119**, 120 (2019). DOI: 10.1021/acs.chemrev.8b00172.
21. P. Pattanayak, S. Saha, T. Chatterjee, and B. C. Ranu, *Chem. Commun.* **61**, 247 (2025). DOI: 10.1039/D4CC05127K.
22. X. Wang, L. Kong, S. Zhou, C. Ma, W. Lin, X. Sun, D. Kirsanov, A. Legin, H. Wan, and P. Wang, *Talanta* **239**, 122903 (2022). DOI: 10.1016/j.talanta.2021.122903.
23. O. S. Oluwafemi, S. Parani, T. C. Lebepe, and R. Maluleke, *Green Proce. Synth.* **10**, 805 (2021). DOI: 10.1515/gps-2021-0075.
24. R. Ameta, J. P. Bhatt, and S. C. Ameta, *Quantum Dots: Fundamentals, Synthesis and Applications* (Amsterdam, Netherlands, Elsevier, 2022).
25. M. M. Rahman, F. a. D. M. Opo, and A. M. Asiri, *J. Biomed. Nanotech.* **17**, 2153 (2021). DOI: 10.1166/jbn.2021.3181.
26. J. W. Cleveland, J. I. Choi, R.-S. Sekiya, J. Cho, H. J. Moon, S. S. Jang, and C. W. Jones, *ACS Appl. Mat. Interf.* **14**, 11235 (2022). DOI: 10.1021/acsami.1c21738.
27. S. S. M. Rodrigues, D. S. M. Ribeiro, J. X. Soares, M. L. C. Passos, M. L. M. F. S. Saraiva, and J. L. M. Santos, *Coordin. Chem. Rev.* **330**, 127 (2017). DOI: 10.1016/j.ccr.2016.10.001.
28. K. Samanta, P. Deswal, S. Alam, M. Bhati, S. A. Ivanov, S. Tretiak, and D. Ghosh, *ACS Nano* **18**, 24941 (2024). DOI: 10.1021/acsnano.4c05638.
29. J. Gupta and P. Rajamani, *Envir. Sci. Pollut. Res.* **30**, 48300 (2023). DOI: 10.1007/s11356-023-25356-3.
30. E. a. A. Fadhil and M. M. Abdullah, *Iraqi J. Phys.* **17**, 26 (2019). DOI: 10.30723/ijp.v17i43.472.
31. H. R. Humud, M. M. Abdullah, and D. M. Khudhair, *Iraqi J. Phys.* **12**, 127 (2019). DOI: 10.30723/ijp.v12i25.313.
32. S. K. Mustafa, R. K. Jamal, and K. A. Aadim, *Iraqi J. Sci.* **60**, 2168 (2019). DOI: 10.24996/ijs.2019.60.10.10
33. E. a. A. Fadhil and M. M. Abdullah, *Iraqi J. Sci.* **61**, 1645 (2020). DOI: 10.24996/ijs.2020.61.7.12.
34. J. Sakizadeh, J. P. Cline, M. A. Snyder, C. J. Kiely, and S. Mcintosh, *ACS Appl. Nano Mat.* **5**, 2293 (2022). DOI: 10.1021/acsanm.1c03997.
35. W. Wang, M. Zhang, Z. Pan, G. M. Biesold, S. Liang, H. Rao, Z. Lin, and X. Zhong, *Chem. Rev.* **122**, 4091 (2022). DOI: 10.1021/acs.chemrev.1c00478.

## تخليق النقاط الكمومية (L-cysteine-CdSe) لتطبيقات الاستشعار الحيوي البصري

ذلفاء رشيد عجيل<sup>1</sup>، منال مدحت عبد الله<sup>1</sup> وفاضل محمد لفته<sup>2</sup>

<sup>1</sup> قسم الفيزياء، كلية العلوم، جامعة بغداد، بغداد، العراق

<sup>2</sup> قسم علوم الحياة، كلية العلوم، جامعة بغداد، بغداد، العراق

### الخلاصة

تم تصنيع بلورات نانوية من CdSe ، معدلة باستخدام L-cysteine القابل للذوبان في الماء والمعروفة باسم بلورات نانوية من CdSe/Cys ، باستخدام L-cysteine كعامل تثبيت. تضمنت عملية التصنيع هذه تكوين بلورات نانوية عالية الاستقرار ذات خصائص مرغوبة لتطبيقات مختلفة. تم توصيف بلورات النانو من CdSe/Cys بدقة باستخدام مجموعة من التقنيات التحليلية المتقدمة للحصول على رؤية شاملة حول خصائصها البنيوية والتركيبية والبصرية. تتطابق القمة التي تتوافق مع التوجه المفضل (111) لـ CdSe المغطى بـ L-cysteine مع مكونات اللب المشتركة، كما هو موضح بواسطة انماط XRD. من ناحية أخرى، فإن القمم عند (220) و (311) ليست بارزة. تم إجراء مطيافية التألق الضوئي (PL) لدراسة الخصائص البصرية لبلورات النانو من CdSe/Cys. أظهرت أطياف PL انبعاثاً قوياً للفلورسنت، مما يدل على الكفاءة الكمومية العالية لهذه البلورات النانوية. كانت قمة الانبعاث حادة ومحددة جيداً، مما يسلط الضوء على التوحيد في حجم وتكوين البلورات النانوية المصنعة. تجعل هذه الفلورسنت القوية لبلورات CdSe / Cys النانوية مناسبة لتطبيقات التصوير البيولوجي والاستشعار البيولوجي المختلفة. كشفت الدراسة عن الفلورسنت القوي لجسيمات CdSe / Cys النانوية الكروية، بمتوسط قطر 2.3 نانومتر. أدى تعديل سطح جسيمات CdSe النانوية بالسيستين إلى تحسين قابليتها للذوبان في الماء وتوافقها البيولوجي.

**الكلمات المفتاحية:** النقاط الكمومية لسيلينيد الكادميوم، السيستين، المستشعرات الحيوية، المواد النانوية، الخصائص البصرية.